Quantifying the intrinsic mechanical flexibility of crystalline materials

Meha Bhogra
Theoretical Sciences Unit, Jawaharlal Nehru Centre for Advanced Scientific Research, Jakkur, Bangalore 560 064, India and Department of Mechanical Engineering, Shiv Nadar University, Gautam Budh Nagar, Uttar Pradesh-201314, India

Andrew L. Goodwin
Inorganic Chemistry Laboratory, University of Oxford, South Parks Road, Oxford OX1 3QR, United Kingdom

Anthony K. Cheetham
Materials Research Laboratory, University of California, Santa Barbara, California 93106, USA

Umesh V. Waghmare*
Theoretical Sciences Unit, Jawaharlal Nehru Centre for Advanced Scientific Research, Jakkur, Bangalore 560 064, India

(Received 14 September 2023; accepted 16 November 2023; published 19 December 2023)

The flexibility of a solid reflects its ability to accommodate reversible changes in size or shape. While the term is commonly used in describing physical and biological systems, a quantitative measure and hence the fundamental understanding of flexibility are presently lacking. Drawing on the phenomenology of flow in liquids, we introduce here a measure of intrinsic flexibility of crystalline materials as the fractional release of elastic stress or strain energy through symmetry-constrained internal structural rearrangements. This metric distinguishes robustly the concept of flexibility from that of compliance. Using first-principles density functional theory calculations, we determine the flexibility of four key systems spanning a range of elastic stiffness and underlying chemistries. We find flexibility arises not only from large structural rearrangements associated with soft phonons, but also from hard phonons that couple strongly to strain fields. Our flexibility measure enables high-throughput screening of materials databases to identify next-generation ultraflexible material.

DOI: 10.1103/PhysRevB.108.214106

I. INTRODUCTION

Flexibility is a term used widely, if loosely, to describe the ability of a system to maintain structural integrity whilst accommodating changes in shape, size, or its form in response to external perturbations. On a macroscopic scale, a given material may be made more or less flexible by the way it is processed; such is the basis of many thin film technologies for flexible displays and wearable devices. Flexible materials may be easily bent, stretched, or twisted; this extrinsic flexibility can be quantified in purely geometric terms [1]. However, the concept makes intuitive sense at the atomic scale, too. Flexibility of proteins, for example, represents their tendency to sample different conformational states without varying their chemical connectivity [2,3], or exhibit deformability at each of the residues [4]. Likewise, the so-called "flexibility window" of zeolites refers to the surprisingly large range of densities that can be accommodated in a single material through collective rotations of tetrahedral building units [5,6]. In structural engineering, flexibility is considered complementary to stiffness, a property that resists deformation or deflection of an object to applied loads [7]. A related quantity is the modulus of resilience [8]—a crucial design parameter for springs—computed as the ratio of yield strength and square of the elastic modulus.

There have been many techniques to quantify the flexibility and rigidity of materials—Lagrange's introduction of constraints and Maxwell's counting degrees of freedom [9,10], mathematical rigidity theory, graph theoretic approaches [11], and pebble counting [12]—largely involving bond networks that consist of distance constraints between atoms in the structure. While these approaches are applicable to generic structures that have no special symmetries or geometric singularities, there is no generally accepted measure of intrinsic flexibility for crystalline solids. A particular complication is that crystal symmetry introduces degeneracies that cannot be accounted for in a straightforward manner [13]. The vernacular use of flexibility complicates matters further—in that the term means different things to different authors. The famous metal-organic framework (MOF) known as MOF-5, for instance, has been described at once as both "exceptionally rigid" [14] and possessing "a high degree of flexibility" [15]. Indeed, in the MOF field—where flexibility is of particular importance—the vagueness of what is meant by the term is of enduring concern [16–18].

One approach to understanding structural flexibility is through an intuitively analogous physical property of the liquid state—namely flowability [19,20]. It arises from the large number of internal degrees of freedom that allow a

*waghmare@jncasr.ac.in

liquid to rearrange easily when subjected to external strains, maintaining at once both local atomic coordination and global symmetry. A crystalline solid, by contrast, possesses a well-defined translational periodicity and space-group symmetry that together constrain the degrees of freedom of its constituent atoms. This results in a finite rigidity, reflected in the nonvanishing slope of the transverse acoustic phonon branches [21] and the emergence of a restoring force against external mechanical perturbations. The nonzero elastic moduli of crystals mean that they accumulate large structural stresses in response to mechanical strains, eventually leading to plastic deformation (as in ductile metals) or rupture (as in brittle solids). An alternative mechanism of elastic softening, that circumvents structural failure and phase transformation, is through the activation of certain normal modes, that is, internal structural rearrangements reminiscent of those involved in liquid flow. It is this component that, we will come to argue, captures the essence of intrinsic flexibility of crystals [Fig. 1(a)].

In this study, we address the straightforward question of how to quantify flexibility in crystalline materials, and the obvious corollary of how then to tune it. Our approach proceeds as follows. First we present our quantitative measure of intrinsic flexibility in crystals as the fractional release of strain energy or elastic stress through symmetry-preserving atomic displacements of the homogeneously deformed crystal **C**. Considering hydrostatic and shear strains as prototypic perturbations of reference crystal $\mathbf{C}_{\text{ref}}$, we determine the flexibility of four key solids spanning a range of chemistries: wurtzitic ZnO, the negative thermal expansion (NTE) material ZrW_2O_8 [22], MOF-5 [15], and another canonical MOF known as ZIF-8 [23] (refer to the Supplemental Material [24] for their structural details). By decomposing this flexibility metric into its contributions from different normal modes of **C**, we show that it is maximized in systems where there is a cooperative effect involving both low- and high-energy modes. The former are the soft phonons often invoked in conventional descriptions of mechanical flexibility, but the latter are also crucial because they couple strongly to strain and so absorb the stresses generated during crystal deformation. This normal-mode analysis allows us to express flexibility as an interplay of elastic stiffness, on the one hand, and degree of strain-phonon coupling on the other hand. Extending the analysis to symmetry-breaking structural changes, we formally derive the nonlinear flexibility due to a lattice mode at any generic wave vector.

II. THE CONCEPT OF LINEAR FLEXIBILITY

As flagged above, we associate mechanical flexibility of a crystalline solid with its ability to accommodate homogeneous deformation without a phase transition or loss of structural integrity. Analysis of linear flexibility, applicable to small deformations, becomes physically transparent and simple if a given mode of deformation is decoupled from the rest at the lowest order. To this end, we consider $\vec{\epsilon}_\mu$, the μ^{th} eigenvector that diagonalizes the 6×6 matrix of symmetric elastic modulus tensor, represented in Voigt notation: $[\epsilon_{xx}\ \epsilon_{yy}\ \epsilon_{zz}\ 2\epsilon_{yz}\ 2\epsilon_{xz}\ 2\epsilon_{xy}]$, with ϵ_{ii} and ϵ_{ij} $(i \neq j)$ as the normal and shear components, respectively. For example, hydrostatic

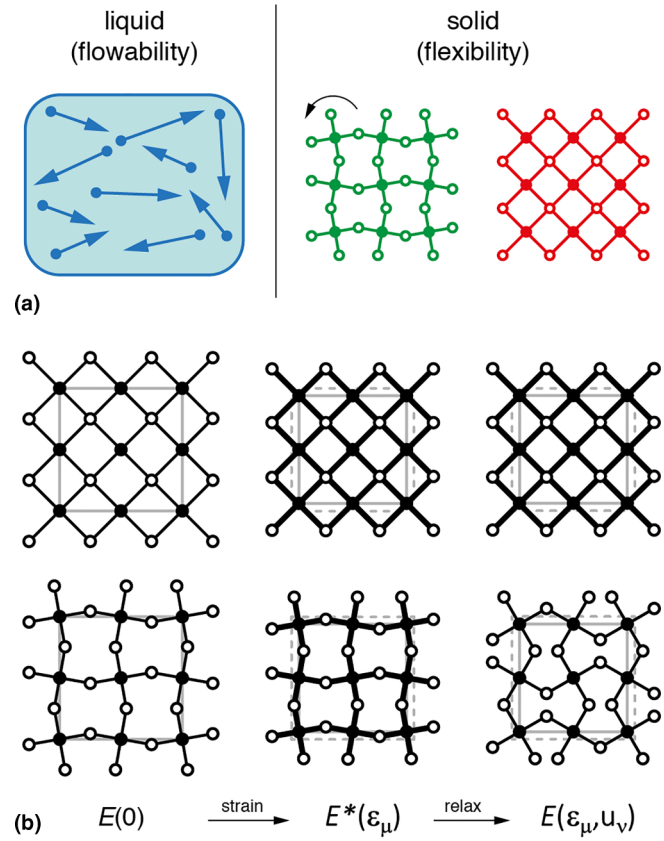

FIG. 1. Flexibility and its determination in crystalline materials. (a) The flowability of a liquid arises from the large number of internal rearrangements possible whilst preserving its global symmetry. The breaking of its continuous symmetry associated with the transition to the crystalline state results in elastic stiffness; whether or not continuous symmetry-preserving distortions persist depends on the particular crystal symmetry. Here the green structure has one such distortion mode, but the red structure has none. (b) To quantify the flexibility of crystals, we determine the energy in three states: minimum-energy ground state with ϵ=0 (left), strained without internal relaxation (center), and after relaxation (right). The flexibility f is given by the fraction of strain energy that is released on subsequent relaxation. Here, one has $f = 0$ for the inflexible system (top) and $0 < f < 1$ for the flexible system (bottom). Note that the relaxation step in the latter case involves both correlated rotations of the square units and bond stretches.

strain ϵ in cubic crystals is $\vec{\epsilon}_h = \epsilon[1\ 1\ 1\ 0\ 0\ 0]$, and $\vec{\epsilon}_r = 2\gamma[0\ 0\ 0\ 1\ 1\ 1]$ gives a the rhombohedral strain γ. To quantify flexibility, we define a dimensionless parameter $f \in [0, 1]$ as follows:

$$f(\vec{\epsilon}_\mu) = \frac{E^*(\vec{\epsilon}_\mu) - \underset{\vec{d}}{\text{Min}}\{E(\vec{\epsilon}_\mu, \vec{d})\}}{E^*(\vec{\epsilon}_\mu) - E(0,0)}, \tag{1}$$

where $E^*(\vec{\epsilon}_\mu)$ and $E(\vec{\epsilon}_\mu)$ [Fig. 1(b)] are the energies of crystal **C** under uniform strain mode $\vec{\epsilon}_\mu$ determined, respectively, without relaxation (clamped structure) and on energy-minimization through relaxation of atomic positions: $E^*(\vec{\epsilon}_\mu) = E(\vec{\epsilon}_\mu, 0)$. On minimization of energy of a crystal **C** strained with $\vec{\epsilon}_\mu$, atomic positions $\{\vec{r}_i\}$ in the $\mathbf{C}_{\text{ref}}$, undergo displacements $\{\vec{d}_i\}$, resulting in a structure with atomic positions $\{\vec{R}_i\}$. All three states—unstrained, strained, and subsequently

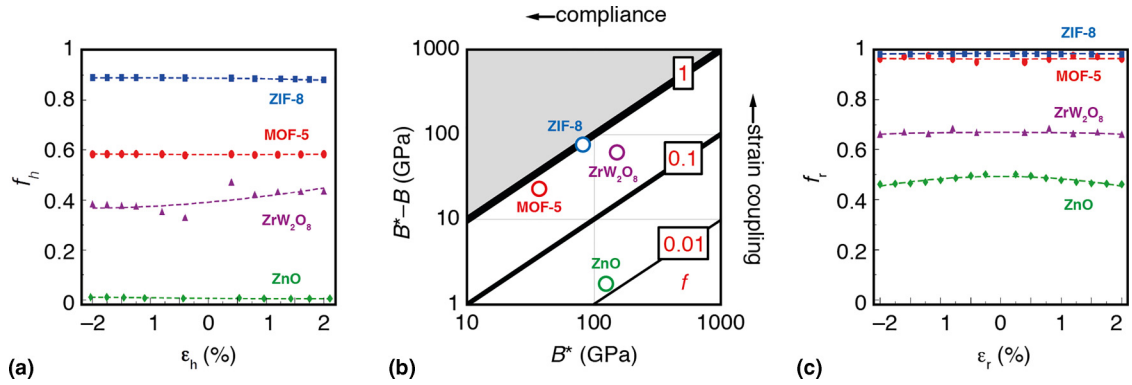

FIG. 2. Flexibility of four key materials determined using DFT. (a) Variation of f_h with applied hydrostatic strain ϵ_h for each of the four systems discussed in the text. (b) Ashby plot of material flexibility (diagonal lines) in terms of its contributions from bare bulk modulus B^* and difference in bare and conventional bulk moduli B^*-B. Note that the most compliant systems are not necessarily the most flexible. (c) Flexibilities determined under rhombohedral shear strain (subscript "r").

relaxed—share the same symmetry. This is valid at low temperatures as long as the thermal vibrations do not disrupt the space-group symmetry of the crystal.

The set of N 3D vectors, $\{\vec{d}_i\}$ can be represented as a $(3N\times1)$ vector $\Delta\vec{s} = d_{l\alpha}$, where $d_{l\alpha} = R_{l\alpha}$-$r_{l\alpha}$, $r_{l\alpha}$, and $R_{l\alpha}$ being the reduced (crystal) position coordinates of the l^{th} atom in the $\boldsymbol{\alpha}$ direction of relaxed and unrelaxed structures, respectively. f is thus the fractional release of strain energy of affinely deformed crystal $\mathbf{C}$ due to internal structural rearrangement that minimizes E w.r.t. displacements $\{\vec{d}_i\}$, maintaining its space-group symmetry $\mathbf{G}$. The projections $\{u\}$ of $\Delta\vec{s}_\mu$ onto its normal modes $\{\hat{e}_{q=0}\}$ are nonzero only for the set of modes $\{\hat{e}_\nu\}$ that preserve the symmetry of the crystal $\mathbf{C}$ with strain ϵ_μ. For any crystal with no symmetry-preserving internal degrees of freedom (e.g., NaCl or body-centered cubic metals), the energies before and after relaxation are identical and $f = 0$. These are crystals with no intrinsic linear flexibility. The other extremum ($f \sim 1$) describes systems in which a large fraction of energy cost associated with homogeneous strain $\vec{\epsilon}$ is released or recovered through symmetry-preserving internal reorganization. These crystals are soft and have a high degree of intrinsic flexibility.

In the harmonic approximation, the elastic strain energy $E(\vec{\epsilon}_\mu, \vec{d}_i)$, in terms of the homogeneous strain component ϵ_μ and projections of internal displacements $\{u_\nu\}$, is

$$E(\epsilon_\mu, \{u_\nu\}) = \frac{1}{2}VC^*_\mu\epsilon^2_\mu + \sum_{\nu=1}^{n}\left(g_{\mu\nu}\epsilon_\mu u_\nu + \frac{1}{2}K_\nu u^2_\nu\right), \quad (2)$$

where V is volume of the equilibrium crystal. The sum is taken over the modes ν that preserve the symmetry of the deformed crystal along ϵ_μ, with spring constant K_ν (obtained from the eigenspectrum of the force-constant matrix), and first-order strain-phonon coupling strength $g_{\mu\nu}$. C^*_μ is the μ^{th} eigenvalue of bare elastic modulus tensor of the reference crystal $\mathbf{C}_{\text{ref}}$, with corresponding eigenvector $\vec{\epsilon}_\mu$. C^*_μ is the modulus that quantifies stiffness or resistance to affine deformation [25] along ϵ_μ with no internal structural relaxation.

Minimization of $E(\epsilon_\mu)$ in Eq. (2) with respect to u_ν gives $u^{(\min)}_\nu = \frac{-g_{\mu\nu}\epsilon_\mu}{K_\nu}$, and hence, $f_{\mu\nu} = \frac{1}{V}\frac{(g_{\mu\nu})^2}{K_\nu C^*_\mu}$. This allows us to describe the flexibility parameter f in terms of scaled internal displacements $\partial u_\nu/\partial\epsilon_\mu$ along normal modes ν:

$$f^L_\mu = \sum_{\nu=1}^{n} f_{\mu\nu} = \frac{1}{V}\sum_{\nu=1}^{n}\frac{K_\nu}{C^*_\mu}\left(\frac{\partial u_\nu}{\partial\epsilon_\mu}\right)^2. \quad (3)$$

This indicates that the variations in K_ν and $(\partial u_\nu/\partial\epsilon_\mu)^2$ amongst different modes are important, and their cooperative effects on the competition with C^*_μ dictate f_μ, up to first order.

III. FLEXIBILITY: RESULTS AND DISCUSSION

To illustrate the concepts presented in Eq. (1), we determined the value of f for the four crystalline solids ZnO, ZrW_2O_8, MOF-5, and ZIF-8 using density functional theory (DFT) calculations (refer to Ref. [24] and the references therein, for computational details). Focusing initially on hydrostatic strains ($\vec{\epsilon}_{ii}$ or $\vec{\epsilon}_h$), our results are shown in Fig. 2(a) for a range of small strains $-0.02 \leqslant \epsilon \leqslant 0.02$. The dense nonporous material ZnO has a nonzero intrinsic flexibility, albeit with a very small value; this is entirely consistent with intuition. But our metric f_h now quantitatively ranks the flexibility of the three open-framework materials ZrW_2O_8, MOF-5, and ZIF-8. Of these, ZrW_2O_8 and MOF-5 show intermediate flexibilities, with the inorganic framework slightly less flexible than the MOF. But, perhaps surprisingly, the difference in f_h between these two frameworks is less than that between MOF-5 and ZIF-8; indeed, we find the latter is remarkably close to the $f = 1$ limit. Note that, for a given system, f_h is essentially independent of ϵ_h in the linear regime. The small asymmetric response of ZrW_2O_8 is an artifact of its nonlinear elastic behavior (i.e., strain derivatives of the elastic modulus) and anharmonic contributions to its strain energy $E(\vec{\epsilon}_h, \{u_\nu\})$ (see Ref. [24] for details).

We now understand why these different crystals have different intrinsic flexibilities under hydrostatic strains, and what makes one more flexible than the other. To answer this, we reformulate Eq. (1) in terms of relaxed and unrelaxed bulk moduli:

$$f_h = \frac{B^* - B}{B^*}. \quad (4)$$

This signifies that flexibility emerges as a competition between the role of internal displacements in the elastic response

TABLE I. Bulk moduli, flexibilities, and numbers of symmetry-preserving normal modes (n) of the crystals considered in this study. Earlier reported values for B and the corresponding references are given in parentheses.

	B (GPa)	B^*(GPa)	f	n
ZnO	126.6 (129.7 [30])	128.3	0.01	1
ZrW_2O_8	94.9 (104.3 [31])	154.8	0.39	11
MOF-5	15.8 (17.0 [32])	38.2	0.59	9
ZIF-8	9.5 (7.8 [33])	83.8	0.89	18

(B^*-B) and the underlying stiffness of the material (B^*) in the absence of such displacements. We note here that B is related to elastic modulus as $B = (1/3)(C_{11} + 2C_{12})$, the eigenvalue corresponding to $\vec{\epsilon}_h$. Experimentally, B^* can be measured using Brillouin scattering, while B represents the static elastic modulus and is typically obtained from the equation of state in variable-pressure diffraction measurements [26].

In Table I, we report the values of B and B^* determined from our DFT calculations for each of the four systems we study here. ZnO is essentially inflexible since B^* is large and (B^*-B) is very small. ZrW_2O_8 is more flexible—despite a larger B^*—because its structure exhibits significant elastic softening in response to homogeneous strains. Although MOF-5 is about six times more compliant than ZrW_2O_8 (lower B^*), it is only slightly more flexible because structural relaxation plays a similar relative role in accommodating strains in the two materials. Finally, ZIF-8 emerges as the most flexible material not because its B^* value is the smallest (it's not), but because B^* and B are so very different [Fig. 2(b)]. Note the distinction that emerges between compliance (inverse of stiffness) and flexibility: a material can be stiff yet flexible (e.g., ZrW_2O_8), or compliant yet inflexible (e.g., body-centered cubic $Cs_{(s)}$, $B \sim 2$ GPa [27], $f = 0$). Nevertheless, the general relationship $B = (1 - f)B^*$ reflects the collective intuition [28,29] that increased flexibility is generally linked with softer elastic moduli (B in the present case).

Since the crystal symmetry is maintained with hydrostatic strains $\vec{\epsilon}_h$, the number of symmetry-preserving modes n remains the same as in $\mathbf{C}_{\text{ref}}$, shown in Table I. Because the individual $f_{h\nu}$ terms for each mode are necessarily positive, one might naïvely expect f_h to scale with n. This turns out to be mostly true, but not always so: the counterexample being that MOF-5 has fewer symmetry-preserving modes than ZrW_2O_8 yet is the more flexible (Table I). Hence, we must determine the contributions of individual modes to identify the key microscopic mechanisms crucial for intrinsic flexibility f_h. The various values of $f_{h\nu}$, K_ν, and $\partial u_\nu/\partial \epsilon_h$ for the symmetry-preserving modes of each material system are enumerated in Tables S2–S4 of Ref. [24] and represented schematically in Fig. 3(a). As anticipated, we find that the relative magnitudes of $f_{h\nu}$ vary enormously from mode to mode, such that for each material f_h is in fact dominated by just one or two modes—quite unexpectedly with relatively large spring constants—that nonetheless couple strongly to hydrostatic strain ϵ_h. By contrast, the atomic displacements associated with flexibility arise from a low-energy mode for which $f_{h\nu}$

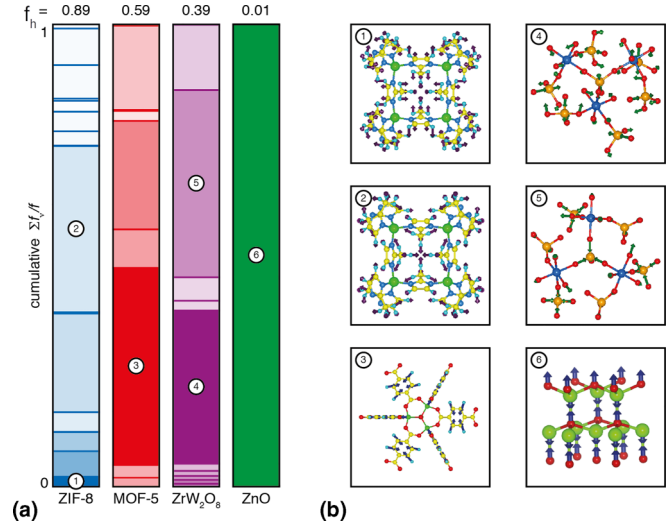

FIG. 3. Key flexibility modes in ZIF-8, MOF-5, ZrW_2O_8, and ZnO. (a) Flexibility due to dominant modes in each of the four materials considered in our study. In each panel, the blocks are arranged by increasing K_ν values, and colored according to the mode displacement (dark = large displacement); the height $f_{h\nu}/f_h$ of each block corresponds to the fractional contribution of a mode ν to flexibility f_h of the material. For the various systems, the mode(s) that contribute most strongly to f_h and/or correspond to the largest displacements are assigned a number label. (b) Representations of the six labeled modes identified in (a).

need not be particularly large. In the case of ZIF-8, there is a clear distinction between these two contributions: the lowest-energy symmetry-preserving mode dominates internal atomic displacements, while the corresponding elastic strain energy is absorbed essentially by higher-energy modes. MOF-5 and ZrW_2O_8 are rather different in that the softest modes (lowest K_ν) do not permit large structural rearrangements with strain (low $\partial u_\nu/\partial \epsilon_h$). The atomic displacements correspond to somewhat higher-energy modes and so have smaller absolute magnitudes. ZnO possesses a single symmetry-preserving mode that couples very weakly to strain, which is why its value of f_h is so low. A key result of our analysis is that structural flexibility embodies contributions from both hard and soft symmetry-preserving vibrations—in contrast to the widely held view that flexibility has its origin solely in low-frequency modes [23,34].

The collection of modes that dominate structural rearrangements, on the one hand, and strain-energy absorption, on the other hand, are illustrated for each of our four materials in Fig. 3(b). In the case of ZIF-8, the key displacement mode ($\omega \sim 1.4$ THz) involves the concerted rotations of methyl-imidazolate linkers that open up the sodalite four-ring windows; this is the "swing mode" implicated in the unusual adsorption and high-pressure response [35] of this framework. At the same time, strain energy is absorbed by a high-energy mode that involves bond stretching in the building units of the crystal [36]. Both effects are associated with the same mode in MOF-5: a collective deformation of the whole SBU-linker-SBU struts that includes squeezing of the central benzene ring. In ZrW_2O_8, displacements are dominated by coupled translations of the WO_4 tetrahedron

pairs along the cell diagonal; this mode has been identified elsewhere as key to the pressure-induced amorphization [37], negative thermal expansion (NTE), and negative hydration expansion (NHE) [38] of the material. Again, as expected, higher-energy bond stretches absorb most of the strain energy. The single symmetry-preserving mode ($\omega \sim 13.2$ THz) in ZnO describes the free parameter between the interpenetrating *hcp* sublattices along the c direction.

We now extend our discussion on flexibility of crystals in response to a generic strain eigenvector $\vec{\epsilon_\mu}$. While for the hydrostatic strain, the symmetry of $\mathbf{C}_{\rm ref}$ is the same as that of $\mathbf{C}$, the nonhydrostatic strains manifest as a deformed crystal $\mathbf{C} = \bar{\boldsymbol{D}}\mathbf{C}_{\rm ref}$, typically with a lower symmetry (see Ref. [24] for details). Here, $\bar{\boldsymbol{D}}$ is the deformation-gradient tensor corresponding to the relevant eigenvector. Transformation of $\mathbf{C}_{\rm ref}$ in accordance with the irreducible representation matrix (or symmetry label) isomorphic to $\bar{\boldsymbol{D}}$ maps it onto the deformed crystal $\mathbf{C}$. The lower the symmetry of $\mathbf{C}$, the larger the set of symmetry-preserving modes in $\mathbf{C}$. Hence, one expects increased flexibility under nonhydrostatic strains, a point borne out by our calculations: we show in Fig. 2(c) the off-diagonal values $f_{\rm r}$ for each of the four materials under rhombohedral strain $\vec{\epsilon_r} = 2\gamma[0\ 0\ 0\ 1\ 1\ 1]$. Now, ZnO becomes moderately flexible, while the increase in flexibility observed for MOF-5 under shear is quite spectacular. This arises from (i) C^*_{44} lower than B^*, (29.7 vs 38.2 GPa; see Table S5), and (ii) the vast increase in the number of symmetry-preserving degrees of freedom in shear-deformed crystals $\mathbf{C}$ (89 for MOF-5 in $R\bar{3}m$ vs 9 in $Fm\bar{3}m$). The modes responsible for this increased flexibility are again a combination of high-energy rigid-unit distortions and large-amplitude soft modes, as highlighted in Fig. S3 of Ref. [24]. That symmetry-lowering increases flexibility has long been recognized in an heuristic sense [39], but our analysis now allows this dependency finally to be quantified. Interestingly, the converse of this finding, that is, rendering a structure more symmetric makes it less flexible, has been highlighted recently in a MOF crystal wherein structural transition from triclinic to monoclinic results in a fully locked rigid structure through minimization of its flexibility [40].

IV. GENERALIZATION: NONLINEAR FLEXIBILITY

Foregoing analysis of the linear mechanical flexibility of materials applies to small deformations and release of elastic strain energy while maintaining the space-group symmetry of deformed crystal. Nonetheless, some flexible frameworks undergo internal structural deformations while deviating from their parent symmetry as a function of pressure or temperature [41], involving reversible changes in the structure modulated over several periodic unit cells. In such cases, the lattice mode ν at a generic wave vector q ($q \neq 0$) contributes to the corresponding internal displacements $\vec{d}_i$. The strain energy E in terms of their projection, u, on a mode $\{\hat{e}_{\nu,q\neq 0}\}$ is

$$E(\epsilon_\mu, u_\nu) = \frac{1}{2}C_\mu V\epsilon_\mu^2 - g'\epsilon_\mu\frac{u^2}{2} + \frac{1}{2}k'u^2 + \frac{\alpha}{4}u^4, \quad (5)$$

where, the first term is elastic strain energy of the relaxed structure, as determined from Eq. (2), and other terms represent the origin of release of additional strain energy possible due to symmetry-breaking internal strains u. k' and α are harmonic and quartic spring constants of the mode $\hat{e}_\nu$, and $g' > 0$ is its second-order coupling with strain ϵ_μ. Note that g' is related to the Gruneisen parameter. We note that the linear coupling between ϵ_μ and u is zero due to symmetry constraint. For $g'\epsilon_\mu < u'$, our analysis of linear flexibility applies. For $g'\epsilon_\mu > k'$, minimization of Eq. (5) with respect to u gives

$$u_{\rm min} = \left(\frac{g'\epsilon_\mu - k'}{\alpha}\right)^{\frac{1}{2}}. \quad (6)$$

Substituting $u_{\rm min}$ in Eq. (5), we obtain

$$E(\epsilon_\mu) = \frac{1}{2}\left(C_\mu V - \frac{g'^2}{2\alpha}\right)\epsilon_\mu^2 + \frac{1}{2\alpha}(g'k')\epsilon_\mu - \frac{k'^2}{4\alpha}. \quad (7)$$

At the critical strain $\epsilon_\mu = \frac{k'}{g'}$, $E = \frac{1}{2}C_\mu V(\frac{k'}{g'})^2$, the strain energy corresponds to the limit of symmetry-preserving structural change.

Beyond the critical strain, the structure destabilizes. For $\epsilon_\mu > \frac{k'}{g'}$, the slope of strain energy with respect to ϵ_μ is

$$\left.\frac{\partial E}{\partial \epsilon_\mu}\right|_{\epsilon_\mu > \frac{k'}{g'}} = \left(C_\mu V - \frac{g'^2}{2\alpha}\right)\epsilon_\mu + \frac{g'k'}{2\alpha} = C_\mu V\epsilon_\mu. \quad (8)$$

Thus, the strain energy E and its first derivative are continuous at the critical strain, $\epsilon_c = \frac{k'}{g'}$, similar to a second-order phase transition in crystals. Nonlinear mechanical flexibility thus involves reversible phase changes. For strains, $\epsilon_\mu < 0$ with $g' < 0$, the same analysis follows. Combining Eqs. (4) and (8), it is evident that the elastic modulus decreases by $\frac{g'^2}{2V_o\alpha}$ due to symmetry-breaking structural changes. The overall flexibility for $\epsilon > \epsilon_c$ is

$$f_\mu = \left(\frac{g_{\mu\nu}^2}{K_\nu} + \frac{g'}{2\alpha}\right)\frac{1}{V_o C_\mu^*}, \quad (9)$$

which shows that linear (first term) and nonlinear (second term) contributions to flexibility arise from linear and second-order coupling of phonons with elastic strain.

Temperature dependence of the flexibility parameter, as introduced here, emerges from anharmonic interactions among phonons, which are also responsible for thermal expansion and lattice thermal conductivity. Typically, thermal expansion of a crystal results in small changes in its cell volume, and its impact on bare elastic moduli (through nonlinear elasticity) is expected to be weak. On the other hand, contributions of optical phonons (atomic relaxation) to relaxed elastic moduli are expected to exhibit temperature dependence originating from temperature induced softening of their frequencies. These phonon frequencies approach small values as the crystal approaches its melting temperature. This further results in larger internal displacements in crystals at elevated temperatures, hence an increase in flexibility due to lattice anharmonicity and thermal fluctuations. This correlates with softening of the lattice as the elastic moduli decrease with temperature. We note that the linear dependence of flexibility on temperature is an approximation and is expected to saturate to values less than one. Second, if there is a structural phase transition, an anomaly in flexibility or nonmonotonous dependence on temeperature is expected near the transition temperature.

V. CONCLUSIONS

We have proposed a quantitative measure of mechanical flexibility, and uncovered its origin in crystalline materials. While mechanical rigidity of a crystal originates from spontaneously broken continuous translational and rotational symmetries of the liquid state, the concept of flexibility is physically quite profound in a way that it counters this rigidity through continuous internal symmetry-preserving degrees of freedom. Our generalization to nonlinear flexibility shows that reversible, symmetry-lowering deformations that break the periodicity of the crystal involves physical mechanisms akin to second-order phase transitions. The idea of flexibility is thus extendible to any long-range ordered state arising from broken-continuous symmetry, including electronic polarization or magnetization, with electric or magnetic field as the external perturbation. A key advantage of our approach to quantifying flexibility is that there is now a clear and straightforward mechanism by which one can identify the most interesting systems using materials databases: all the necessary information is contained within the elastic tensor C—usually already available—and its constrained analog C^* related to affine deformation, which is straightforward to calculate.

ACKNOWLEDGMENTS

We acknowledge National Supercomputing Mission (NSM), Jawaharlal Nehru Centre for Advanced Scientific Research (JNCASR) for providing access to computational facilities. U.V.W. acknowledges support from a J.C. Bose National Fellowship of SERB-DST, Government of India. A.L.G. acknowledges the European Research Council (Grant No. 788144). M.B. acknowledges the India-Korea Joint Network Centre for Computational Materials Science, funded by the Department of Science and Technology, Government of India.

[1] J. Peng and G. J. Snyder, A figure of merit for flexibility, Science **366**, 690 (2019).
[2] B. Schulze, A. Sljoka, and W. Whiteley, How does symmetry impact the flexibility of proteins? Philos. Trans. R. Soc. A **372**, 20120041 (2014).
[3] J. Janin and M. J. K. Sternberg, Protein flexibility, not disorder, is intrinsic to molecular recognition, F1000 Biol. Rep. **5**, 2 (2013).
[4] J. A. Kovacs, P. Chacón, and R. Abagyan, Predictions of protein flexibility: First-order measures, Proteins **56**, 661 (2004).
[5] A. Sartbaeva, S. A. Wells, M. M. J. Treacy, and M. F. Thorpe, The flexibility window in zeolites, Nat. Mater. **5**, 962 (2006).
[6] S. A. Wells and A. Sartbaeva, GASP: software for geometric simulations of flexibility in polyhedral and molecular framework structures, Mol. Simul. **41**, 1409 (2015).
[7] P. Nagarajan, *Matrix Methods of Structural Analysis (1st ed.)* (CRC Press, Boca Raton, 2018).
[8] M. Kaltenbrunner, M. S. White, E. D. Głowacki, T. Sekitani, T. Someya, N. S. Sariciftci, and S. Bauer, Ultrathin and lightweight organic solar cells with high flexibility, Nat. Commun. **3**, 770 (2012).
[9] J. C. Maxwell, L. On the calculation of the equilibrium and stiffness of frames, Lond. Edinb. Dublin philos. mag. j. Sci. **27**, 294 (1864).
[10] A. Marmier and K. E. Evans, Flexibility in MOFs: do scalar and group-theoretical counting rules work? Dalton Trans. **45**, 4360 (2016).
[11] M. Thorpe, M. Lei, A. Rader, D. J. Jacobs, and L. A. Kuhn, Protein flexibility and dynamics using constraint theory, J. Mol. Graphics Modell. **19**, 60 (2001).
[12] D. J. Jacobs, A. J. Rader, L. A. Kuhn, and M. F. Thorpe, Protein flexibility predictions using graph theory, Proteins **44**, 150 (2001).
[13] A. P. Giddy, M. T. Dove, G. S. Pawley, and V. Heine, The determination of rigid-unit modes as potential soft modes for displacive phase transitions in framework crystal structures, Acta Crystallogr. A **49**, 697 (1993).
[14] M. Eddaoudi, J. Kim, N. Rosi, D. Vodak, J. Wachter, M. O'Keeffe, and O. M. Yaghi, Systematic design of pore size and functionality in isoreticular MOFs and their application in methane storage, Science **295**, 469 (2002).
[15] D. Dubbeldam, K. Walton, D. Ellis, and R. Snurr, Exceptional negative thermal expansion in isoreticular metal–organic frameworks, Angew. Chem. Int. Ed. **46**, 4496 (2007).
[16] T. D. Bennett, A. K. Cheetham, A. H. Fuchs, and F.-X. Coudert, Interplay between defects, disorder and flexibility in metal–organic frameworks, Nat. Chem. **9**, 11 (2017).
[17] S. Horike, S. Shimomura, and S. Kitagawa, Soft porous crystals, Nat. Chem. **1**, 695 (2009).
[18] J. H. Lee, S. Jeoung, Y. G. Chung, and H. R. Moon, Elucidation of flexible metal-organic frameworks: Research progresses and recent developments, Coord. Chem. Rev. **389**, 161 (2019).
[19] L. Bocquet, A. Colin, and A. Ajdari, Kinetic theory of plastic flow in soft glassy materials, Phys. Rev. Lett. **103**, 036001 (2009).
[20] A. Widmer-Cooper, H. Perry, P. Harrowell, and D. R. Reichman, Irreversible reorganization in a supercooled liquid originates from localized soft modes, Nat. Phys. **4**, 711 (2008).
[21] C. P. Goodrich, A. J. Liu, and S. R. Nagel, Solids between the mechanical extremes of order and disorder, Nat. Phys. **10**, 578 (2014).
[22] T. A. Mary, J. S. O. Evans, T. Vogt, and A. W. Sleight, Negative thermal expansion from 0.3 to 1050 kelvin in ZrW_2O_8, Science **272**, 90 (1996).
[23] A. Schneemann, V. Bon, I. Schwedler, I. Senkovska, S. Kaskel, and R. A. Fischer, Flexible metal-organic frameworks, Chem. Soc. Rev. **43**, 6062 (2014).
[24] See Supplemental Material at http://link.aps.org/supplemental/10.1103/PhysRevB.108.214106 for the structural details of the crystals used in this study; computational details; asymmetry of f_h in ZrW_2O_8 with hydrostatic strain; relative contributions

of symmetry-preserving modes to flexibility f of crystals upon hydrostatic and rhombohedral shear strains; and eigenvectors of symmetry-preserving modes that are dominant contributors to flexibility of shear-deformed crystals. The Supplemental Material also contains Refs. [22,42–46].

[25] Q. Wen, A. Basu, P. A. Janmey, and A. G. Yodh, Non-affine deformations in polymer hydrogels, Soft Matter **8**, 8039 (2012).

[26] T. S. Duffy, G. Shen, J. Shu, H.-K. Mao, R. J. Hemley, and A. K. Singh, Elasticity, shear strength, and equation of state of molybdenum and gold from x-ray diffraction under non-hydrostatic compression to 24 gpa, J. Appl. Phys. **86**, 6729 (1999).

[27] F. Kollarits and J. Trivisonno, Single-crystal elastic constants of cesium, J. Phys. Chem. Solids **29**, 2133 (1968).

[28] A. U. Ortiz, A. Boutin, A. H. Fuchs, and F.-X. Coudert, Anisotropic elastic properties of flexible metal-organic frameworks: How soft are soft porous crystals? Phys. Rev. Lett. **109**, 195502 (2012).

[29] Z. Zhang, Y. Yang, E. S. Penev, and B. I. Yakobson, Elasticity, flexibility, and ideal strength of borophenes, Adv. Funct. Mater. **27**, 1605059 (2017).

[30] C. Fan, Q. Wang, L. Li, S. Zhang, Y. Zhu, X. Zhang, M. Ma, R. Liu, and W. Wang, Bulk moduli of wurtzite, zinc-blende, and rocksalt phases of ZnO from chemical bond method and density functional theory, Appl. Phys. Lett. **92**, 101917 (2008).

[31] F. R. Drymiotis, H. Ledbetter, J. B. Betts, T. Kimura, J. C. Lashley, A. Migliori, A. P. Ramirez, G. R. Kowach, and J. Van Duijn, Monocrystal elastic constants of the negative-thermal-expansion compound zirconium tungstate (ZrW_2O_8), Phys. Rev. Lett. **93**, 025502 (2004).

[32] M. Mattesini, J. M. Soler, and F. Ynduráin, Ab initio study of metal-organic framework-5 $Zn_4O(1,4-\text{benzenedicarboxylate})_3$: An assessment of mechanical and spectroscopic properties, Phys. Rev. B **73**, 094111 (2006).

[33] K. W. Chapman, G. J. Halder, and P. J. Chupas, Pressure-induced amorphization and porosity modification in a metal-organic framework, J. Am. Chem. Soc. **131**, 17546 (2009).

[34] D. Fairen-Jimenez, S. Moggach, M. Wharmby, P. Wright, S. Parsons, and T. Düren, Opening the gate: framework flexibility in ZIF-8 explored by experiments and simulations, J. Am. Chem. Soc. **133**, 8900 (2011).

[35] S. A. Moggach, T. D. Bennett, and A. K. Cheetham, The effect of pressure on ZIF-8: Increasing pore size with pressure and the formation of a high-pressure phase at 1.47 GPa, Angew. Chem. Int. Ed. **48**, 7087 (2009).

[36] J. Eckert, High energy phonons: overview, Tech. Rep. LA–10227-C-Vol2 (1984), proceedings of the 1984 workshop on high-energy excitations in condensed matter. Vol. II, http://inis.iaea.org/search/search.aspx?orig_q=RN:17008325.

[37] D. A. Keen, A. L. Goodwin, M. G. Tucker, M. T. Dove, J. S. O. Evans, W. A. Crichton, and M. Brunelli, Structural description of pressure-induced amorphization in ZrW_2O_8, Phys. Rev. Lett. **98**, 225501 (2007).

[38] M. Baise, P. M. Maffettone, F. Trousselet, N. P. Funnell, F.-X. Coudert, and A. L. Goodwin, Negative hydration expansion in ZrW_2O_8: microscopic mechanism, spaghetti dynamics, and negative thermal expansion, Phys. Rev. Lett. **120**, 265501 (2018).

[39] S. J. Hunt, M. J. Cliffe, J. A. Hill, A. B. Cairns, N. P. Funnell, and A. L. Goodwin, Flexibility transition and guest-driven reconstruction in a ferroelastic metal–organic framework, CrystEngComm **17**, 361 (2014).

[40] D. Jędrzejowski, M. Pander, W. Nitek, W. Bury, and D. Matoga, Turning flexibility into rigidity: Stepwise locking of interpenetrating networks in a mof crystal through click reaction, Chem. Mater. **33**, 7509 (2021).

[41] A. Nearchou, M.-L. U. Cornelius, Z. L. Jones, I. E. Collings, S. A. Wells, P. R. Raithby, and A. Sartbaeva, Pressure-induced symmetry changes in body-centred cubic zeolites, R. Soc. Open Sci. **6**, 182158 (2019).

[42] O. M. Yaghi, M. O'Keeffe, N. W. Ockwig, H. K. Chae, M. Eddaoudi, and J. Kim, Reticular synthesis and the design of new materials, Nature (London) **423**, 705 (2003).

[43] J. S. O. Evans, W. I. F. David, and A. W. Sleight, Structural investigation of the negative-thermal-expansion material ZrW_2O_8, Acta Crystallogr. B: Structural Science **55**, 333 (1999).

[44] G. Kresse and J. Furthmüller, Efficient iterative schemes for ab initio total-energy calculations using a plane-wave basis set, Phys. Rev. B **54**, 11169 (1996).

[45] D. Vanderbilt, Soft self-consistent pseudopotentials in a generalized eigenvalue formalism, Phys. Rev. B **41**, 7892 (1990).

[46] J. P. Perdew, K. Burke, and M. Ernzerhof, Generalized gradient approximation made simple, Phys. Rev. Lett. **77**, 3865 (1996).